2018

Adenosine has two faces: Regionally dichotomous adenosine tone in a model of epilepsy with comorbid sleep disorders

Ted J. Warren

Timothy A. Simeone

D. David Smith

Ryan Grove

Jiri Adamec

See next page for additional authors

Authors

Ted J. Warren, Timothy A. Simeone, D. David Smith, Ryan Grove, Jiri Adamec, Kaeli K. Samson, Harrison M. Roundtree, Deepak Madhavan, and Kristina A. Simeone

HHS Public Access

Author manuscript

Neurobiol Dis. Author manuscript; available in PMC 2020 November 04.

Published in final edited form as:

Neurobiol Dis. 2018 June ; 114: 45–52. doi:10.1016/j.nbd.2018.01.017.

Adenosine has two faces: Regionally dichotomous adenosine tone in a model of epilepsy with comorbid sleep disorders

Ted J. Warren[a], **Timothy A. Simeone**[a], **D. David Smith**[b], **Ryan Grove**[c], **Jiri Adamec**[c], **Kaeli K. Samson**[a,d], **Harrison M. Roundtree**[a], **Deepak Madhavan**[e], **Kristina A. Simeone**[a,*]

[a]Department of Pharmacology, Creighton University School of Medicine, Omaha, NE 68178, United States

[b]Department of Biomedical Sciences, Creighton University School of Medicine, Omaha, NE 68178, United States

[c]Department of Biochemistry and Redox Biology Center, University of Nebraska - Lincoln, Lincoln, NE 68588, United States

[d]Department of Biostatistics, University of Nebraska Medical Center, Omaha, NE 68198, United States

[e]Department of Neurological Sciences, Nebraska Comprehensive Epilepsy Program, University of Nebraska Medical Center, Omaha, NE 68198, United States

Abstract

Objective: Adenosine participates in maintaining the excitatory/inhibitory balance in neuronal circuits. Studies indicate that adenosine levels in the cortex and hippocampus increase and exert sleep pressure in sleep-deprived and control animals, whereas in epilepsy reduced adenosine tone promotes hyperexcitability. To date, the role of adenosine in pathological conditions that result in both seizures and sleep disorders is unknown. Here, we determined adenosine tone in sleep and seizure regulating brain regions of $K_v1.1$ knockout (KO) mice, a model of temporal epilepsy with comorbid sleep disorders.

Methods: 1) Reverse phase-high performance liquid chromatography (RP-HPLC) was performed on brain tissue to determine levels of adenosine and adenine nucleotides. 2) Multi-electrode array extracellular electrophysiology was used to determine adenosine tone in the hippocampal CA1 region and the lateral hypothalamus (LH).

Results: RP-HPLC indicated a non-significant decrease in adenosine (~50%, $p = 0.23$) in whole brain homogenates of KO mice. Regional examination of relative levels of adenine nucleotides indicated decreased ATP and increased AMP in the cortex and hippocampus and increased adenosine in cortical tissue. Using electrophysiological and pharmacological techniques, estimated

*Corresponding author at: 2500 California Plaza, Omaha, NE 68178, United States. kristinasimeone@creighton.edu (K.A. Simeone).

Author contributions

KAS, DM, & TAS contributed to the concepts and study design. TJW, KKS, HMR, DDS, JA, RG, TAS, KAS contributed to experiments, data acquisition, and analysis. TJW, TAS, & KAS wrote and edited the manuscript.

Conflict of interest

The authors have no conflicts of interest.

adenosine levels were ~35% lower in the KO hippocampal CA1 region, and 1–2 fold higher in the KO LH. Moreover, the increased adenosine in KO LH contributed to lower spontaneous firing rates of putative wake-promoting orexin/hypocretin neurons.

Interpretation: This is the first study to demonstrate a direct correlation of regionally distinct dichotomous adenosine levels in a single model with both epilepsy and comorbid sleep disorders. The weaker inhibitory tone in the dorsal hippocampus is consistent with lower seizure threshold, whereas increased adenosine in the LH is consistent with chronic partial sleep deprivation. This work furthers our understanding of how adenosine may contribute to pathological conditions that underlie sleep disorders within the epileptic brain.

Keywords

Mitochondria; Kv1.1 knockout; Cerebral cortex; Hippocampus; Lateral hypothalamus

1. Introduction

Persistent disturbances in sleep architecture and quality are commonly associated with many neurological and psychiatric disorders, including epilepsy (St. Louis, 2011; Krause et al., 2017). Adenosine is a neuromodulator that elicits antiseizure and somnogenic actions. Adenosine tone has an inhibitory effect on excitatory synapses via the adenosine 1 receptor (A_1R) throughout the brain (Dunwiddie, 1980). During temporal lobe seizures, adenosine levels rise which suppresses further seizure activity (Winn et al., 1980). However, in cases of chronic epilepsy this inhibitory mechanism is weakened or lacking as seen in animal models and humans with lower adenosine tone (Rebola et al., 2003; Masino et al., 2011; Boison, 2016; Porkka-Heiskanen et al., 1997). As a somnogen, adenosine levels have been reported to rise in specific cortical, temporal, and subcortical brain regions when wake periods exceed physiological durations (Porkka-Heiskanen et al., 2000; Basheer et al., 2004; Weber and Dan, 2016). Rising adenosine levels are thought to promote sleep by inhibiting neurons involved in wakefulness and cognition; thus, decreased levels may be responsible for sleep disruption (Boison and Aronica, 2015). For individuals with both epilepsy and sleep disruption, a logical, yet untested, hypothesis is that a uniformly reduced adenosine tone underlies both conditions (Boison, 2016).

Here we determined the adenosine tone in $K_v1.1$ knockout (KO) mice, a model of epilepsy with comorbid sleep disorders. KO mice lack the α-subunit of the $K_v1.1$ voltage-gated delayed rectifier potassium channel, have a severe epilepsy phenotype with multiple types of seizures, including frequent generalized tonic-clonic seizures, and present pathology similar to temporal lobe epilepsy (Smart et al., 1998; Wenzel et al., 2007; Simeone et al., 2016). We have recently reported that KO mice also have sleep-disorder symptoms consistent with involvement of the orexin/hypocretin system, including disrupted sleep architecture and insufficient amounts of non-rapid eye movement (NREM) sleep and rapid eye movement (REM) sleep (Roundtree et al., 2016).

Orexin/hypocretin neurons are a subset of wake-promoting neurons located in the lateral hypothalamus (LH). Severe seizures propagate to the LH in KO mice, and the LH displays signs of chronic pathology (including increased blood-brain permeability, astrogliosis and

impaired mitochondrial function) and increased orexin/hypocretin protein levels (Roundtree et al., 2016). Orexin/hypocretin neurons express A_1R and their inhibition is known to promote sleep (Chemelli et al., 1999; Liu and Gao, 2007). Thus, we hypothesized that adenosine concentrations would be lower in KO hippocampus and LH providing a common etiology for ictogenesis in the hippocampus and for the sleep disorders seen in the LH of KO mice. Contrary to our hypothesis, our data indicate regionally divergent adenosine tones in KO brain indicating a hitherto unrecognized complexity in the regulation of adenine nucleotides during complex and chronic neurological disorders.

2. Methods

2.1. Animals

C3HeB/FeJ $K_v1.1$ knockout (KO) and wild-type (WT) littermates were bred, reared, genotyped, and housed as previously described (Roundtree et al., 2016). Mice were entrained to a strict 12 h light/dark cycle with access to food and water ad libitum. Lights on occurred at zeitgeber time (ZT) 00:00 h. For all electrophysiology experiments, mice were sacrificed between 03:00–04:00 ZT to control for diurnal changes in adenosine levels in the brain. Adult male and female mice (5–9 weeks old) were used for these experiments. All experiments conformed to NIH guidelines in accordance with the United States Public Health Service's Policy on Humane Care and Use of Laboratory Animals and were approved by Creighton University's Institutional Animal Care and Use Committee.

2.2. Reversed-phase high pressure liquid chromatography (RP-HPLC) tissue extraction

For RP-HPLC experiments, mice were euthanized using a Muromachi Microwave Fixation System (Model MMW-05, Muromachi Kikai Co., LTD, Tokyo, Japan) in order to quickly (< 1 s) raise the brain temperature above 85 °C and inactivate enzymatic activity. This is necessary in order to prevent post-mortem ATP/ADP/AMP metabolism by nucleotidase activity and accumulation of adenosine as a technical artifact. Mice were initially anesthetized using isoflurane and placed in a restrainer with a water jacket and euthanized (3.5 kW and 0.89 s); (Delaney and Geiger, 1996). The whole brain was removed and examined for proper fixation then immediately placed in 0.1 M sulfuric acid and homogenized on ice. Tris (0.1 M) base was added to homogenized tissue in sulfuric acid followed by 1 M NaOH to neutralize the homogenate. The neutralized homogenate was centrifuged at 15 rcf for 15 min at 4 °C. Supernatant was collected for RP-HPLC (Akula et al., 2008). Adenosine concentrations from whole brains were normalized to protein concentration as determined using the Bradford method performed on a sample of each homogenate.

2.3. HPLC analysis of whole brain tissue

Conversion of adenosine to the N^6-etheno derivative was accomplished by a previously published method (Haink et al., 2003). Briefly, standards or the extraction solution (8 mice total 50 μL) was added to a freshly prepared mixture of chloroacetaldehyde (~50% in water from Aldrich) and sodium acetate buffer (1 M, pH 4.5) (11.2/138.8, v/v, 150 μL). After heating at 60 °C for 1 h, the mixture was cooled in ice water to stop the reaction, filtered through a 0.45 μm membrane and used without dilution for RP-HPLC analysis. RP-HPLC

was performed on a Waters 626 instrument equipped with a 600S controller, a 474 scanning fluorescence detector and a 717plus autosampler. Analysis of etheno-derivatized standards and extracts was performed by a previously published method modified to separate N^6-ethenoadenosine from interfering peaks derived from mouse brain (Bhatt et al., 2012). Separation was achieved on a Waters XTerra MS C_{18} column (3 × 50 mm, 5μm), equipped with a C18 guard cartridge (Phenomenex, Torrance, CA), eluted with mixtures of buffer A (tetrabutylammonium-hydrogensulfate (5.7 mM) and KH_2PO_4 (30.5 mM) adjusted to pH 5.8 with 2 M KOH) and buffer B (acetonitrile/buffer A, 2/1, v/v) at 1.5 mL/min. Samples of the derivatizing mixture (50 μL) were loaded on to the column, which had been previously equilibrated with buffer A. The column was eluted by increasing the percentage of buffer B in the eluent to 40% over 1 min, holding buffer B at 40% for 1.4 min before reducing the percentage of buffer B back to 0% over 0.1 min. The column was then washed with buffer A for 2.5 min before the next sample was loaded. The eluent was continuously monitored for fluorescence employing an excitation wavelength of 280 nm and an emission wavelength of 410 nm (Bhatt et al., 2012). N^6-ethenoadenosine eluted from the column after 1.7 min. Quantification of adenosine amounts was determined using external standards (25–1000 nM, $r^2 = 0.9996$).

2.4. HPLC analysis of adenine nucleotides in specific brain regions

Determination of the concentration of adenine nucleotides followed Levitt et al. (1984). Microwaved fixed brain tissues were homogenized (9 mice total,) in 75% MeOH/0.15 M NaCl to 0.5 mg/mL W/V. The homogenate was combined with 0.15 M NaCl and $CHCl_3$/MeOH (2:1 *v*/v) containing 0.01% BHT. Samples were vortexed for 2 min and phases were allowed to separate for 30 min on ice. After separation, samples were centrifuged for 5 min at 7.8 kg. The lower phase was removed for nonpolar metabolite analysis while the upper, aqueous phase was saved for polar metabolite analysis. To compare adenine nucleotide concentrations, the aqueous portion was converted to its etheno adduct. The aqueous extract was dried under nitrogen then resuspended in a 10:1 (v/v) mixture of Krebs buffer (in mM): 113 NaCl, 4.8 KCl, 2.5 $CaCl_2$, 1.2 KH_2PO_4, 1.2 $MgSO_4$, 25 $NaHCO_3$ and 5.5 glucose) and chloroacetaldehyde. Samples were heated to 80 °C for one hour then cooled to room temperature for HPLC analysis. HPLC consisted of a Shimadzu LC-20AB binary pump connected to a Shimadzu RF-20Axs fluorescent detector. Five μL of the derivatized samples were injected onto an Agilent Eclipse AAA 4.6 × 150 mm column at a flow rate of 0.8 mL/min. Mobile phase A consisted of 0.1% formic acid and mobile phase B consisted of 0.1% formic acid in acetonitrile, and the following gradient was used to separate the adenosine molecules: initial conditions of 0% B was held for 5 min, followed by increases to 4.7% B over 2 min, 11.7% B over 8 min, 35% B over 5 min, 95% B over 5 min then held for 5 min at 95% B. The column was then returned to initial conditions and held for 5 min. Etheno detection was achieved using an excitation wavelength of 300 nm and an emission wavelength of 420 nm. The adenylate energy charge (AEC) was calculated with the following equation:

$$Energy\ charge = \frac{[ATP] + 1/2[ADP]}{[ATP] + [ADP] + [AMP]}$$

2.5. Acute slice preparation and multi-electrode array recordings

WT and KO mice were anesthetized with isoflurane and decapitated. The brains were quickly placed into an ice-cold no Mg^{2+}-sucrose aCSF continuously bubbled with carbogen (95% O_2/5% CO_2) containing (in mM): 206 sucrose, 2.8 KCl, 8 $MgSO_4$, 26 $NaHCO_3$, 1.25 NaH_2PO_4, and 10 glucose, (pH 7.4, Osm 294). Coronal slices (400 μm) were prepared on a Leica VT1200 and transferred to a holding chamber at room temperature (RT) for at least 1 h before recordings. Recordings were taken in an aCSF containing (in mM): 124 NaCl, 2.8 KCl, 2.4 $CaCl_2$, 2.5 $MgSO_4$, 26 $NaHCO_3$, 1.25 NaH_2PO_4, and 25 glucose (pH 7.4, 295 mOsm). Slices were appropriately positioned over the electrode grid of a MED64 probe (Alpha Med Systems, Osaka, Japan; array size: 1 × 1 mm; each electrode: 50 × 50 μm; interpolar distance: 150 μm; 8 × 8 electrode array) and perfused at a rate of 1 mL/min with in-line pre-warmed (~33 °C) aCSF bubbled continuously with carbogen.

2.6. Electrophysiology recording protocols

An electrode in the Schaffer collateral pathway was chosen for stimulation and responses recorded by electrodes in the stratum radiatum of the CA1 (CA1sr) in hippocampal slices (13 mice). For slices containing LH, the medial forebrain bundle fiber tract was stimulated and responses recorded by electrodes in the perifornical area of the LH. An I/O curve was generated for synaptic responses with sequential stimulations (−10 to −180 μA) every 20 s. A stimulation intensity that elicited 40–60% of the maximum output was chosen for experiments and stimulations occurred every 60 s. Field excitatory postsynaptic potentials (fEPSPs) slopes (10–90%) were analyzed. A baseline measurement consisted of at least 10 min of stable recordings before 10 μM of the A_1R antagonist, 2-[4-(2,3,6,7-Tetrahydro-2,6-dioxo-1,3-dipropyl1H-purin-8-yl)phenoxy]-acetic acid (XCC, Tocris) was applied.

For recordings of extracellular action potentials in the LH, spontaneous events from all 64 channels were recorded in continuous, gapfree mode with Mobius software (WitWerx Inc., Tustin, CA) and acquired at a 20 kHz sampling rate with a bandwidth of 10 Hz–10 kHz (7 mice total). Spontaneous activity was recorded from the LH over a period of 5 min. XCC was perfused into the chamber for a period of 10 min before recordings resumed.

2.7. Principal Component Analysis (PCA)

Traces from spontaneous activity within the LH were imported into Spike2(v7) (Cambridge, England) for filtering and PCA to distinguish between principal cells and interneurons. Single unit analysis was carried out according to the specifications in Simeone et al. (2013). Individual traces were filtered with FIR 300–3000 Hz band pass filter. Four times the root mean square (RMS) of the noise of the trace was calculated and served as the threshold for spike detection. After the separation and classification of the units (action potentials) into clusters representing individual neurons, PCA was performed to check precision and refine the initial clustering analysis. Principal cells with a firing frequency below 0.01 Hz were excluded from analysis.

2.8. Estimating local adenosine concentrations

Adenosine concentrations were determined in the hippocampus and the LH following the method of Dunwiddie and Diao (1994). Evoked and spontaneous activity were recorded

before and after a saturating concentration (10 μM) of the A_1 receptor antagonist XCC. The fractional increase (f.i.) of activity was then used to estimate the endogenous adenosine concentration, with the following equation:

$$[Adenosine]_{endogenous} = (f.\ i.)^{1/H} \times EC_{50}$$

where H is the Hill slope (1.52, estimated by Dunwiddie and Diao, 1994), and EC_{50} is the adenosine concentration that produces a half-maximal response (610 nM, estimated by Dunwiddie and Diao, 1994).

2.9. Statistics

All experiments were analyzed with the Student's *t*-test, unless otherwise noted. A p-value < 0.05 was considered statistically significant. All statistical analyses were done using Prism6 software (Graphpad Software, Inc., La Jolla, CA).

3. Results

3.1. Relative adenosine and adenine nucleotide ratios are altered in the KO brain

Initial RP-HPLC experiments indicate similar adenosine levels in whole brain samples from KO mice (by 46.3 ± 14%) and WT mice (Fig. 1; $p = 0.227$). Adenosine exists in a futile regulatory cycle with energy-transfer molecules adenosine triphosphate (ATP), −diphosphate (ADP), and -monophosphate (AMP). To detect regional differences, we determined the relative amounts of adenosine and adenine nucleotides in the hippocampus and cortex. Both WT hippocampus and cortex contained the expected graded ratios of adenine nucleotides with ATP representing the largest proportion (45% ATP, 34% ADP, 20% AMP, and 1% adenosine; Fig. 2A,B) with low coefficient of variations (CV) (Fig. 2C–F). In contrast, KO levels of ATP, ADP, and AMP were similar with large CVs. KO hippocampal proportions were 36% ATP, 30% ADP, and 33% AMP with no change in adenosine (1%). Similarly, KO cortical ratios were 30% ATP, 25% ADP, and 35% AMP, however, adenosine was increased to 10%. The shifting proportions adenine nucleotides resulted in a ~20% decrease in the overall adenylate energy charge in KO brain (Fig. 3). Collectively, these data suggest a dysregulation of energy-storage capacity in KO brain.

3.2. Basal adenosine levels are reduced in KO hippocampus

Electrophysiology and pharmacology was used to determine adenosine tone in local regions that regulate ictogenesis and sleep. First, we tested the hypothesis that adenosine inhibitory tone was reduced in the ictogenic hippocampus. We placed the CA1 region of a hippocampal slice on a 64-electrode array, stimulated the Schaffer collaterals and recorded extracellular dendritic field potentials in the CA1sr (Fig. 4A–C). KO fEPSP 10–90% slopes were 19 ± 2% smaller than WT slopes ($p < 0.167$). Application of a saturating concentration of the A_1R antagonist, XCC (10 μM) increased fEPSP slopes significantly in both WT and KO slices. Antagonizing A_1Rs increased the field potential slope by 35.5 ± 5% in WT CA1sr and 19.3 ± 5% in KO CA1sr ($p < 0.0001$, Fig. 4D). From these fractional increases, an estimate of endogenous adenosine was calculated (see Methods; Dunwiddie and Diao, 1994;

Sandau et al., 2016). Adenosine levels in CA1sr were 35.4 ± 4% lower in KO when compared to WT CA1sr ($p < 0.05$, Fig. 4E) suggesting a weaker inhibitory tone in the KO hippocampus.

3.3. Basal adenosine levels are increased in the KO LH

Increased orexinergic tone was implicated in the sleep disorders of KO mice since an orexin receptor antagonist improved sleep (Roundtree et al., 2016). We tested the hypothesis that adenosine inhibitory tone was reduced in the orexin-rich LH. LH slices were placed on a 64-electrode array, the medial forebrain bundle fiber tract, which runs through the LH, was stimulated and extracellular field potentials in the perifornical area of the LH were recorded (Fig. 5A, B). Units were identified as belonging to single neurons using PCA, and principal cells or interneurons were distinguished based on their spike width and asymmetry (Fig. 5B, C). KO field potential 10–90% slopes were 30.7 ± 10.8% smaller than WT slopes. Following A_1R inhibition with XCC (10 μM), WT field potential slopes increased by 7.9 ± 1.2% compared to an 18.1 ± 2.9% increase of KO slopes; both values were significantly different from baseline (WT $p < 0.0001$; KO $p < 0.0001$) and from each other (WT v. KO $p < 0.001$; Fig. 5D). The estimated adenosine tone in the LH of KO mice was 84.6 ± 1.9% greater than WT (Fig. 5E, $p < 0.001$). In addition, XCC restored KO field potentials to near WT values (Fig. 5D, $p = 0.15$) suggesting that the smaller KO postsynaptic responses are partially due to increased adenosine-mediated inhibition.

Interneurons and orexin neurons in the LH are spontaneously active (Schöne et al., 2011; Karnani et al., 2013) (Fig. 5B), therefore, effects of XCC on action potential firing rates provide another method to determine endogenous adenosine concentrations. Using the multi-electrode array, we performed extracellular recordings of spontaneous action potentials (or units) in electrodes in the perifornical-LH. Interneurons accounted for 93.0% of the WT LH activity and 87.4% of KO activity. There was no statistical difference between the spontaneous firing rates of interneurons between the genotypes ($p = 0.42$) and XCC did not alter firing rates (WT: $p = 0.13$; KO: $p = 0.71$). In contrast, KO principal cells, or putative orexin neurons, fired at 20.3 ± 7% of the rate of their WT littermates ($p = 0.03$; Fig. 5F). The average fractional increase of the firing frequency with XCC was 43.9 ± 12% in WT and 97.9 ± 38% in KO LH following bath application with the A_1R antagonist (Fig. 5F WT, $p = 0.001$; KO, $p = 0.002$). Similar to the field potential findings, this resulted in adenosine concentrations that were higher (192.8 ± 72%) in KO LH compared to WT levels (Fig. 5G; $p < 0.05$). Collectively, these data indicate that adenosine is 1–2 fold higher in KO LH contrary to our original hypothesis.

4. Discussion

The current study is the first to measure adenosine levels in the sleep-promoting LH and is the first to determine adenosine levels in seizure-genic and sleep-related brain regions in a single model of epilepsy with comorbid sleep disorders. First, we present evidence that overall energy charge storage in adenine nucleotides is decreased throughout the brain, supporting our previous findings of widespread mitochondrial dysfunction in regions including the cortex, hippocampus, and hypothalamus (Roundtree et al., 2016; Simeone et

al., 2014; Kim et al., 2015). Second, we demonstrate and confirm that hippocampal adenosine decreases in epilepsy (Rebola et al., 2003; Boison, 2016; Li et al., 2007). Third, and most importantly, our data indicate adenosine increases in the sleep-promoting epileptic cortex and lateral hypothalamus.

Physiological concentrations of adenosine serve as neuromodulators in the hippocampus that contribute to appropriate excitatory/inhibitory balance (Cunha, 2016). Intense neuronal activity during seizures causes the release of ATP from glia and synaptic vesicles which is subsequently broken down to adenosine by ectonucleotidases. The increase of extracellular adenosine aids in limiting excessive excitability and can contribute to the termination of a seizure by hyperpolarizing neurons via A_1R activation and subsequent ion channels (Masino et al., 2011). However, in the epileptic hippocampus, numerous studies (in murine, rat, and human) demonstrate upregulation of adenosine kinase (ADK), which results in an adenosine deficiency and subsequent cellular and network hyperexcitability (Rebola et al., 2003; Masino et al., 2011; Sandau et al., 2016; Gouder et al., 2004; Aronica et al., 2011; de Groot et al., 2012).

Adenosine's role in sleep is more nuanced. In brain regions involved in promoting wakefulness, such as the basal forebrain, cortex, and even the hippocampus, adenosine increases with the amount of time spent awake exerting inhibitory pressure to drive sleep (Basheer et al., 2004; Weber and Dan, 2016). This natural phenomenon is exacerbated during prolonged or chronic sleep deprivation or restriction, and decreases in adenosine tone may contribute to sleep disorders (Coleman et al., 2006; Hines et al., 2013).

It has been proposed that brain-wide decreases in adenosine may promote hyperexcitability in epilepsy; and contribute to sleep and cognitive comorbidities in epilepsy, Alzheimer's disease, Parkinson's disease, and Amyotrophic Lateral Sclerosis (Boison, 2016). Thus far, the evidence for this possibility relies on findings of increased expression of ADK in brain tissue from human epilepsy, Alzheimer's, Parkinson's, and ALS patients. ADK is upregulated in GFAP-expressing reactive astrocytes and phosphorylates adenosine to AMP. Intracellular and extracellular adenosine levels are in equilibrium via passive equilibrative nucleotide transporters expressed by glia and neurons; thus, increased ADK reduces adenosine. The best evidence that decreases in adenosine can result in multiple phenotypic comorbidities comes from studies of global upregulation of ADK in transgenic (Adk-tg) mice. Adk-tg mice have a 50% reduction of tissue levels of adenosine, spontaneous recurrent seizures, severe learning deficits, altered locomotor control, and sleep deficiencies (Li et al., 2007; Yee et al., 2007; Shen et al., 2011; Shen et al., 2012). The above mentioned expression studies on human resected or postmortem tissue assess only regions subjected to insult or trauma, and not necessarily sleep-regulating regions (which may or may not be damaged). Therefore, it is not known whether adenosine tone is altered in regions relevant to specific comorbidities such as sleep.

In an attempt to provide further evidence for adenosine's role in both epilepsy and sleep comorbidities, the current study used a mouse model of epilepsy with sleep disorders that is not directly related to the adenosinergic system. We found similar levels of ATP, ADP, and AMP in KO mice. Future studies will need to determine whether this reflects changes in

adenosine metabolizing enzymes. However, it has been reported that global mitochondrial dysfunction in ATP-producing complex I of the electron transport chain occurs in the KO cortex, hippocampus, and hypothalamus (Roundtree et al., 2016; Simeone et al., 2014; Kim et al., 2015). Within these regions, complex I is inhibited by excessive reactive oxygen species (ROS) correlating with the wide spread damage in the hippocampus and elsewhere (Wenzel et al., 2007; Roundtree et al., 2016; Simeone et al., 2014; Kim et al., 2015). However, sleep deprivation also induces mitochondrial dysfunction and KO mice are significantly sleep deficient (Roundtree et al., 2016; Ramanathan et al., 2002; Andreazza et al., 2010). Regardless of the precipitating cause of mitochondrial dysfunction, these studies support our current HPLC results which indicate a general decrease of ATP and an accumulation of adenosine in lower energy molecules ADP, AMP, and adenosine. Alternatively, the decreased ATP and increased AMP/ATP ratios could reflect increased usage of ATP, which has been reported to occur during seizures and extended wakefulness (Hardie and Frenguelli, 2007; Dworak et al., 2010).

Although whole brain HPLC suggested overall decreases in KO adenosine, regional HPLC and electrophysiology experiments demonstrated increased adenosine in sleep-related cortex and LH and a reduction in seizure-related hippocampus. One possible explanation may be regional differences in damage. For example, Wenzel et al. (2007) found wide spread cell death and GFAP-expressing reactive astrocytes in the same KO model used herein, specifically in the hippocampus, neocortex, piriform cortex, thalamus, and amygdala consistent with environments resulting in increased ADK. In the LH of KO mice we have found evidence of minor damage, limited to BBB permeability and increased GFAP-expressing reactive astrocytes, but no cell death (Boison, 2016; Roundtree et al., 2016). However, few LH astrocytes actually express GFAP, therefore, even though we observed a doubling, these increases may be relatively inconsequential for ADK expression. Collectively, these results suggest that mitochondrial dysfunction contributes to a decrease in ATP production and that the regional expression of ADK may determine in which areas ATP metabolite adenine nucleotides accumulate. Further studies are warranted to further clarify the relationships between mitochondrial ADP usage-ATP production, and changes in adenosine metabolizing enzymes.

In the hippocampus, the reduced levels of adenosine may have predicted disinhibition and thus larger baseline fEPSPs in the CA1 of KO mice. In contrast, fEPSP were smaller in KO when compared with WT mice. This may be due to the loss of $K_v1.1$ itself, which may cause depolarization of the resting membrane and shunting of excitatory inputs resulting in reduced transmitter release. However, this is unlikely as loss of $K_v1.1$ is associated with increased synaptic strength (Simeone et al., 2013). Alternatively, the Schaffer-collateral axons that were stimulated to produce the fEPSPs rely heavily on ATP for synaptic neurotransmitter release. Reduced mitochondrial production of ATP may contribute to decreased synaptic strength in KO hippocampus (Liotta et al., 2012).

In sleep regulating regions, we found KO adenosine levels were increased, supporting previous associations of sleep deficiency and elevated adenosine. In the LH, A_1Rs are expressed on a subset of principal cells, the wake-promoting orexin neurons that project to arousal nuclei of the reticular activating system, thalamus, basal forebrain, and other cortical

and limbic regions to trigger wakefulness (Thakkar et al., 2002). Consistent with increased adenosine and inhibition of orexin neurons during sleep deprivation, baseline LH field potentials are smaller and baseline firing frequencies of putative orexin neurons are slower in KO LH (Grivel et al., 2005; Matsuki et al., 2015). Further, A_1R antagonism restores these to near WT levels.

While this scenario suggests that sleep would be improved, chronic sleep deficiency persists in KO mice (Iyer et al., 2018). This may be due to the increased number of orexin neurons in KO LH (Roundtree et al., 2016). Even though the activity of orexin neurons is decreased, the net orexinergic output may be increased. This notion is supported by our findings that administration of an orexin receptor antagonist was highly effective at improving sleep and reducing seizures in KO mice (Roundtree et al., 2016). Alternatively, adenosine tone may be reduced in one or more of the other sleep-promoting regions. Another possibility is that the seizures themselves are promoting sleep deficiency. We have reported that severe seizures are able to propagate to the LH of KO mice, thus potentially directly activating wake-promoting circuitry (Roundtree et al., 2016). Further, the subsequent pathology including impaired mitochondrial ATP production may contribute to sleep deficiency. The brain-wide net decrease in adenylate energy charge storage and availability could cause the breakdown of homeostatic stability and result in cellular hyperexcitability, degradation of synaptic precision, and the inability to maintain energy-demanding network oscillations such as REM (Brown et al., 2012; Porkka-Heiskanen, 2013). Indeed, KO mice have significantly less REM than WT mice and REM deficiency strongly correlates with seizure severity (Roundtree et al., 2016). Indeed, KO mice have significantly less REM than WT mice and REM deficiency strongly correlated with seizure severity (Roundtree et al., 2016). The interdependent relationship between seizures and sleep deficiency is complex as each negatively exacerbates the other. We have reported that improving sleep with a melatonin receptor agonist or an orexin receptor antagonist reduces seizures (Roundtree et al., 2016; Fenoglio-Simeone et al., 2009a), and that reducing seizures with the ketogenic diet improves sleep (Iyer et al., 2018; Fenoglio-Simeone et al., 2009b). Future studies are required to untangle sleep deficiency from seizures.

In summary, we have demonstrated that regulation of adenosine tone is regionally diverse in epilepsy with comorbid sleep disorders, thus disproving the assumption that global, uniform changes in adenosine may underlie both syndromes. Whether uniform or dichotomous alterations in adenosine tone occur in other relevant models of epilepsy, Alzheimer's disease, Parkinson's disease, or ALS with sleep or cognitive comorbidities remain unknown, and will need to be determined in future studies. This work furthers our understanding of how adenosine may contribute to pathological conditions that underlie sleep disorders within the epileptic brain and suggests that treatments designed to modify the adenosinergic system may need to be targeted to specific regions.

Acknowledgements

We wish to thank Stephanie Matthews for her technical support. This work was supported by National Institutes of Health (NIH) NS072179 (KAS), NIH NS085389 (TAS), and the Citizens United for Research in Epilepsy Foundation (KAS) and (TAS). This work was also supported by the National Center for Research Resources grant G20RR024001. The content is solely the responsibility of the authors and does not necessarily represent the official

views of the National Center for Research Resources or the National Institutes of Health. Please note, KAS has published under the names K Dorenbos, KA Fenoglio, KA Fenoglio-Simeone, and KA Simeone.

References

Akula KK, et al., 2008 Development and validation of an RP-HPLC method for the estimation of adenosine and related purines in brain tissues of rats. J. Sep. Sci 31, 3139–3147. [PubMed: 18780378]

Andreazza AC, et al., 2010 Mitochondrial complex I activity and oxidative damage to mitochondrial proteins in the prefrontal cortex of patients with bipolar disorder. Arch. Gen. Psychiatry 67, 360–368. [PubMed: 20368511]

Aronica E, et al., 2011 Upregulation of adenosine kinase in astrocytes in experimental and human temporal lobe epilepsy. Epilepsia 52, 1645–1655. [PubMed: 21635241]

Basheer R, et al., 2004 Adenosine and sleep-wake regulation. Prog. Neurobiol 73, 379–396. [PubMed: 15313333]

Bhatt DP, et al., 2012 A sensitive HPLC-based method to quantify adenine nucleotides in primary astrocyte cell cultures. J. Chromatogr. B 889–890, 110–115.

Boison D, 2016 Adenosinergic signaling in epilepsy. Neuropharmacology 104, 131–139. [PubMed: 26341819]

Boison D, Aronica E, 2015 Comorbidities in neurology: is adenosine the common link? Neuropharmacology 97, 18–34. [PubMed: 25979489]

Brown RE, et al., 2012 Control of sleep and wakefulness. Physiol. Rev 92, 1087–1187. [PubMed: 22811426]

Chemelli RM, et al., 1999 Narcolepsy in orexin knockout mice: molecular genetics of sleep regulation. Cell 98, 437–451. [PubMed: 10481909]

Coleman CG, et al., 2006 Dialysis delivery of an adenosine A2A agonist into the pontine reticular formation of C57BL/6J mouse increases pontine acetylcholine release and sleep. J. Neurochem 96, 1750–1759. [PubMed: 16539690]

Cunha RA, 2016 How does adenosine control neuronal dysfunction and neurodegeneration? J. Neurochem 139, 1019–1055. [PubMed: 27365148]

Delaney SM, Geiger JD, 1996 Brain regional levels of adenosine and adenosine nucleotides in rats killed by high-energy focused microwave irradiation. J. Neurosci. Methods 64, 151–156. [PubMed: 8699875]

Dunwiddie TV, 1980 Endogenously released adenosine regulates excitability in the in vitro hippocampus. Epilepsia 21, 541–548. [PubMed: 7418669]

Dunwiddie TV, Diao L, 1994 Extracellular adenosine concentrations in hippocampal brain slices and the tonic inhibitory modulation of evoked excitatory responses. J. Pharmacol. Exp. Ther 268, 537–545. [PubMed: 8113965]

Dworak M, et al., 2010 Sleep and brain energy levels: ATP changes during sleep. J. Neurosci 30, 9007–9016. [PubMed: 20592221]

Fenoglio-Simeone K, et al., 2009a Anticonvulsant effects of the selective melatonin receptor agonist ramelteon. Epilepsy Behav. 16, 52–57. [PubMed: 19682955]

Fenoglio-Simeone KA, et al., 2009b Ketogenic diet treatment abolishes seizure periodicity and improves diurnal rhythmicity in epileptic Kcna1-null mice. Epilepsia 50, 2027–2034. [PubMed: 19490051]

Gouder N, et al., 2004 Overexpression of adenosine kinase in epileptic hippocampus contributes to epileptogenesis. J. Neurosci 24, 692–701. [PubMed: 14736855]

Grivel J, et al., 2005 The wake-promoting hypocretin/orexin neurons change their response to noradrenaline after sleep deprivation. J. Neurosci 25, 4127–4130. [PubMed: 15843615]

de Groot M, et al., 2012 Overexpression of ADK in human astrocytic tumors and peritumoral tissue is related to tumor-associated epilepsy. Epilepsia 53, 58–66.

Haink G, et al., 2003 Liquid chromatography method for the analysis of adenosine compounds. J. Chromatogr. B 784, 189–193.

Hardie DG, Frenguelli BG, 2007 A neural protection racket: AMPK and the GABA(B) receptor. Neuron 53, 159–162. [PubMed: 17224398]

Hines DJ, et al., 2013 Antidepressant effects of sleep deprivation require astrocyte-dependent adenosine mediated signaling. Transl. Psychiatry 3, e212. [PubMed: 23321809]

Iyer SH, et al., 2018 Accumulation of rest deficiency precedes sudden death of epileptic Kv1.1 Knockout Mice, a model of SUDEP. Epilepsia 59, 92–105.

Karnani MM, et al., 2013 Lateral hypothalamic GAD65 neurons are spontaneously firing and distinct from orexin- and melanin-concentrating hormone neurons. J. Physiol 591, 933–953. [PubMed: 23184514]

Kim DY, et al., 2015 Ketone bodies mediate antiseizure effects through mitochondrial permeability transition. Ann. Neurol 78, 77–87. [PubMed: 25899847]

Krause AJ, et al., 2017 The sleep-deprived human brain. Nat. Rev. Neurosci 18, 404–418. [PubMed: 28515433]

Levitt B, et al., 1984 High-pressure liquid chromatographic-fluorometric detection of adenosine and adenine nucleotides: application to endogenous content and electrically induced release of adenyl purines in guinea pig vas deferens. Anal. Biochem 137, 93–100. [PubMed: 6731811]

Li T, et al., 2007 Suppression of kindling epileptogenesis by adenosine releasing stem cell-derived brain implants. Brain 130, 1276–1288. [PubMed: 17472985]

Liotta A, et al., 2012 Energy demand of synaptic transmission at the hippocampal Schaffer-collateral synapse. J. Cereb. Blood Flow Metab 32, 2076–2083. [PubMed: 22929439]

Liu ZW, Gao XB, 2007 Adenosine inhibits activity of hypocretin/orexin neurons by the A1 receptor in the lateral hypothalamus: a possible sleep-promoting effect. J. Neurophysiol. 97, 837–848. [PubMed: 17093123]

Masino SA, et al., 2011 A ketogenic diet suppresses seizures in mice through adenosine A_1 receptors. J. Clin. Invest 121, 2679–2683. [PubMed: 21701065]

Matsuki T, et al., 2015 GABAA receptor-mediated input change on orexin neurons following sleep deprivation in mice. Neuroscience 284, 217–224. [PubMed: 25286384]

Porkka-Heiskanen T, 2013 Sleep homeostasis. Curr. Opin. Neurobiol 23, 799–805. [PubMed: 23510741]

Porkka-Heiskanen T, et al., 1997 Adenosine: a mediator of the sleep-inducing effects of prolonged wakefulness. Science 276, 1265–1268. [PubMed: 9157887]

Porkka-Heiskanen T, et al., 2000 Brain site-specificity of extracellular adenosine concentration changes during sleep deprivation and spontaneous sleep: an in vivo microdialysis study. Neuroscience 99, 507–517. [PubMed: 11029542]

Ramanathan L, et al., 2002 Sleep deprivation decreases superoxide dismutase activity in rat hippocampus and brainstem. Neuroreport 13, 1387–1390. [PubMed: 12167758]

Rebola N, et al., 2003 Decrease of adenosine A1 receptor density and of adenosine neuromodulation in the hippocampus of kindled rats. Eur. J. Neurosci 18, 820–828. [PubMed: 12925008]

Roundtree HM, et al., 2016 Orexin receptor antagonism improves sleep and reduces seizures in Kcna1-null mice. Sleep 39, 357–368. [PubMed: 26446112]

Sandau US, et al., 2016 Adenosine kinase deficiency in the brain results in maladaptive synaptic plasticity. J. Neurosci 36, 12117–12128. [PubMed: 27903722]

Schöne C, et al., 2011 Dichotomous cellular properties of mouse orexin/hypocretin neurons. J. Physiol 589, 2767–2779. [PubMed: 21486780]

Shen HY, et al., 2011 Adenosine kinase determines the degree of brain injury after ischemic stroke in mice. J. Cereb. Blood Flow Metab 31, 1648–1659. [PubMed: 21427729]

Shen HY, et al., 2012 Adenosine augmentation ameliorates psychotic and cognitive endophenotypes of schizophrenia. J. Clin. Invest 122, 2567–2577. [PubMed: 22706302]

Simeone TA, et al., 2013 Loss of the Kv1.1 potassium channel promotes pathologic sharp waves and high frequency oscillations in in vitro hippocampal slices. Neurobiol. Dis 54, 68–81. [PubMed: 23466697]

Simeone KA, et al., 2014 Targeting deficiencies in mitochondrial respiratory complex I and functional uncoupling exerts anti-seizure effects in a genetic model of temporal lobe epilepsy and in a model of acute temporal lobe seizures. Exp. Neurol 251, 84–90. [PubMed: 24270080]

Simeone KA, et al., 2016 Ketogenic diet treatment increases longevity in Kcna1-null mice, a model of sudden unexpected death in epilepsy. Epilepsia 57, e178–82. [PubMed: 27346881]

Smart SL, et al., 1998 Deletion of the K(V)1.1 potassium channel causes epilepsy in mice. Neuron 20, 809–819. [PubMed: 9581771]

St. Louis EK, 2011 Sleep and epilepsy: strange bedfellows no more. Minerva Pneumol. 50, 159–176. [PubMed: 23539488]

Thakkar MM, et al., 2002 Orexin neurons of the hypothalamus express adenosine A1 receptors. Brain Res. 944, 190–194. [PubMed: 12106679]

Weber F, Dan Y, 2016 Circuit-based interrogation of sleep control. Nature 538, 51–59. [PubMed: 27708309]

Wenzel HJ, et al., 2007 Structural consequences of Kcna1 gene deletion and transfer in the mouse hippocampus. Epilepsia 48, 2023–2046. [PubMed: 17651419]

Winn HR, et al., 1980 Changes in brain adenosine during bicuculline-induced seizures in rats. Effects of hypoxia and altered systemic blood pressure. Circ. Res 47, 568–577. [PubMed: 6773698]

Yee BK, et al., 2007 Transgenic overexpression of adenosine kinase in brain leads to multiple learning impairments and altered sensitivity to psychomimetic drugs. Eur. J. Neurosci 26, 3237–3252. [PubMed: 18005073]

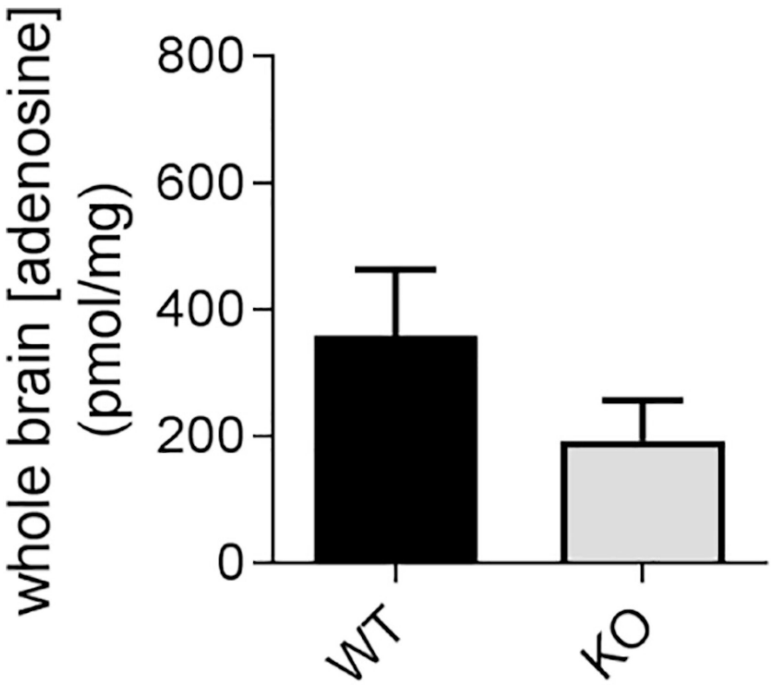

Fig. 1.

Whole brain adenosine levels in KO and WT mice.

Focal microwave irradiation ensured fidelity of endogenous adenosine levels by limiting enzymatic activity within the tissue. Adenosine concentrations of whole brain were normalized to the protein concentration from their respective samples (WT 358 ± 105 pmol/mg; KO 192 ± 65 pmol/mg). Data are mean ± SEM, $n = 3–5$.

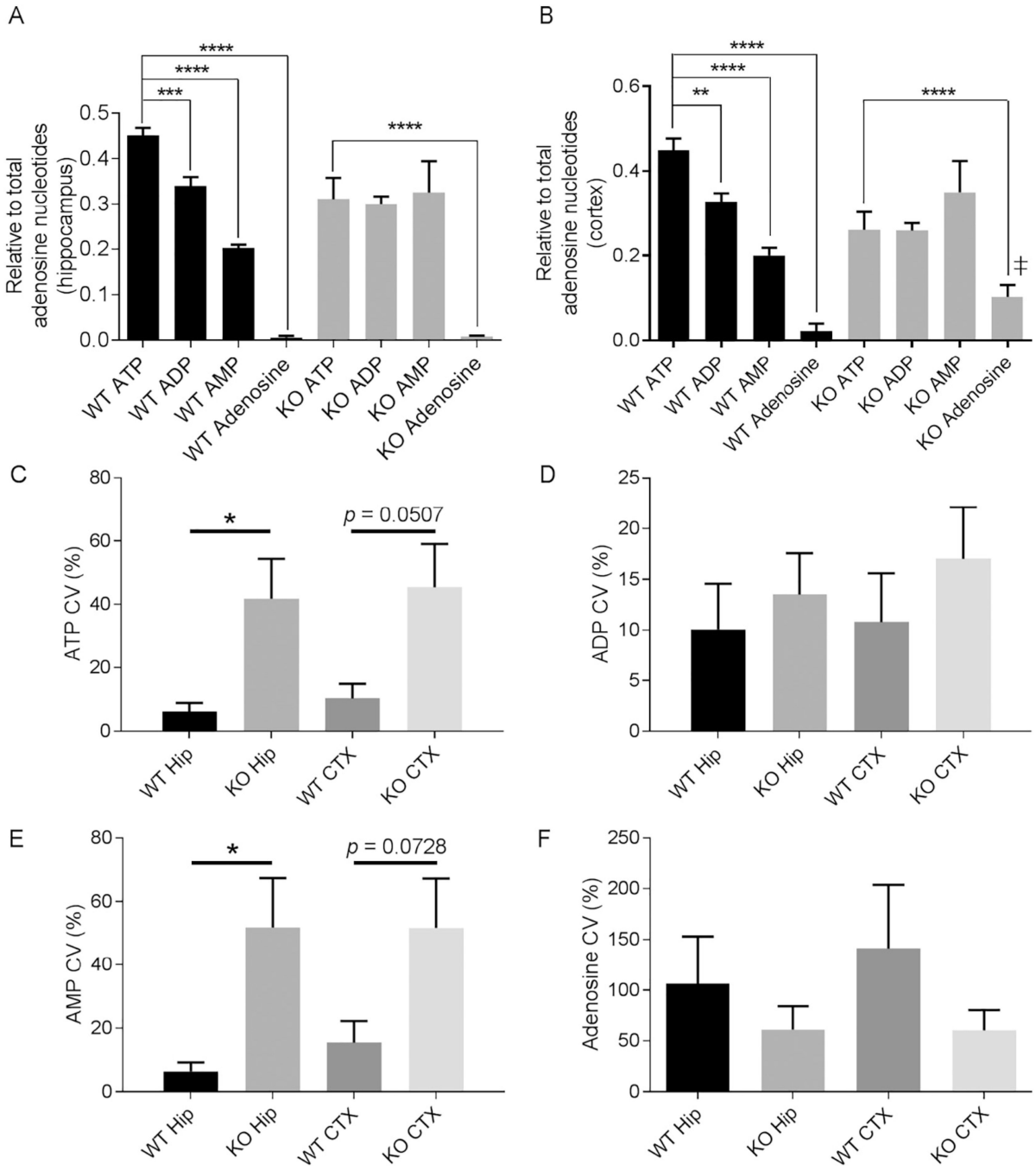

Fig. 2.

Adenosine energy transfer molecules differ in KO hippocampus and cortex when compared to WT.

(A) The respective ratios of ATP, ADP, AMP, and adenosine relative to the total adenosine metabolite concentration in the hippocampi of WT and KO mice (WT: $F(3,7)= 85.27$; KO: $F(3, 18) = 6.688$, one-way ANOVA with Dunnett's multiple comparison test). **(B)** Ratios from cortex (WT: $F(3, 8) = 75.39$; KO: $F(3, 18) = 4.514$, one-way ANOVA with Dunnett's multiple comparison test). **(C-F)** Individual coefficient of variation (CV) (as %) in the

hippocampus (hip) and cortex (CTX) for **(C)** ATP, **(D)** ADP, **(E)** AMP and **(F)** adenosine; n=3 WT and 6 KO mice. Data analyzed with an unpaired *t*-test with Welch's correction.

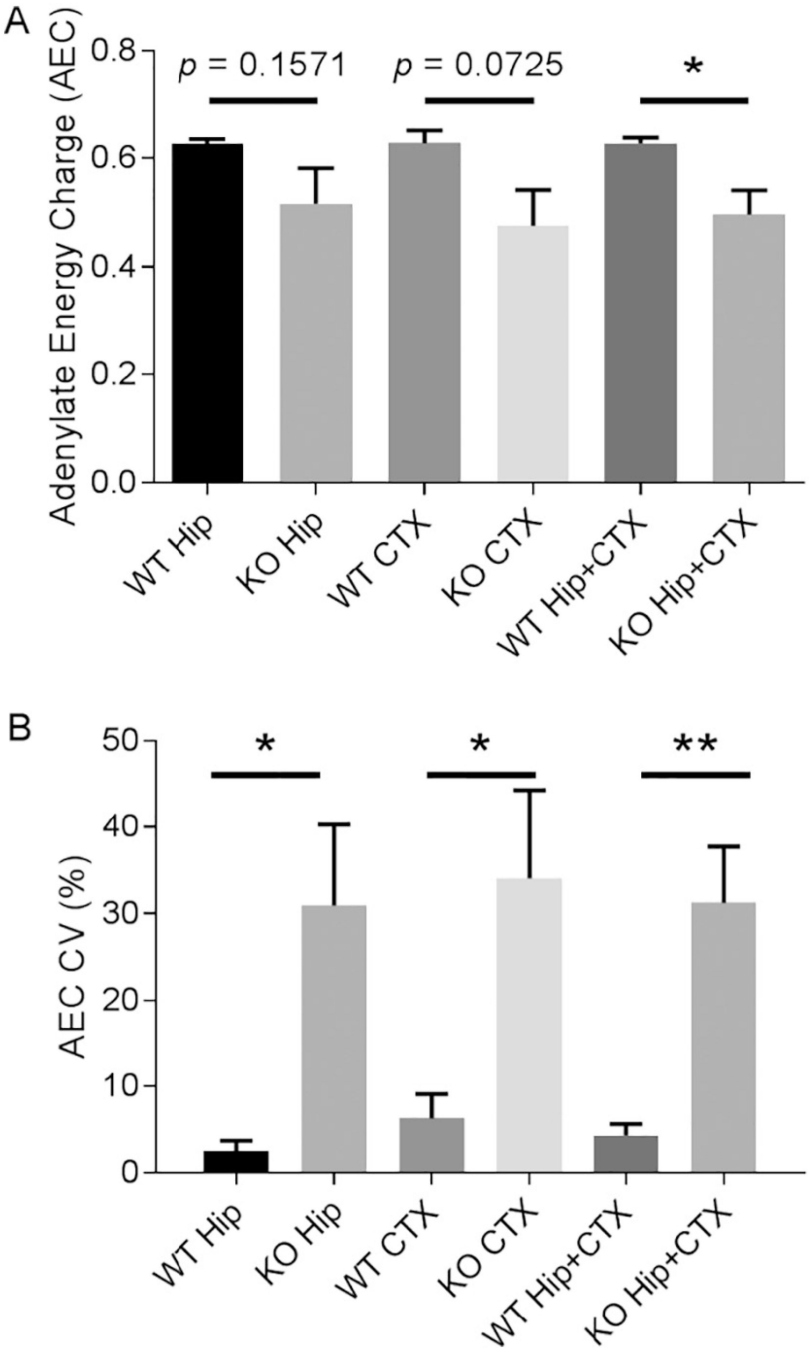

Fig. 3.

Significant variance in the AEC of KO mice.

(A) The adenylate energy charge (AEC) of WT and KO hippocampus (Hip), cortex (CTX) and combined (Hip+CTX). **(B)** The mean coefficient of variation (CV) of AEC is comparatively larger in both the hippocampus and cortex of the KO mice, n = 3 WT and 6 KO mice. Data analyzed using an unpaired t-test with Welch's correction.

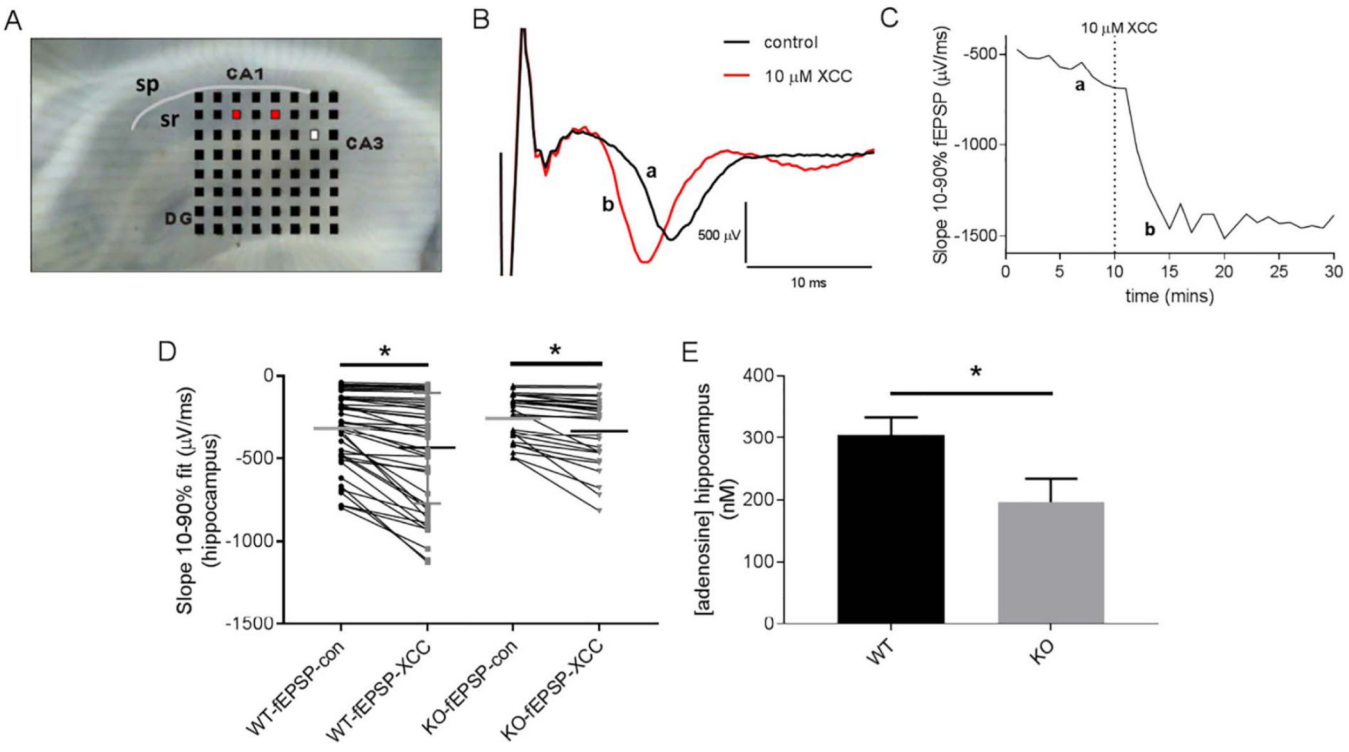

Fig. 4.

Synaptic adenosine levels are lower in the CA1sr of the hippocampus in KO mice.

(A) Image of hippocampus from a coronal slice centered over an 8 × 8 multielectrode array. MFs were stimulated with an electrode in CA2 (white). Recordings were taken from the sr in CA1 (sp indicated by grey line). **(B)** Example fEPSPs from CA1 pyramidal neurons before **(a)** and after **(b)** 10 μM XCC. The slope represents the strength of the postsynaptic response from stimulation of the MFs (note the increase of negativity of the slope after A_1R inhibition). **(C)** Example measurement of the slopes of the fEPSP after stimulation every minute before **(a)** and after **(b)** 10 μM XCC. **(D)** Individual fEPSP values before and after 10 μM XCC in WT and KO mice. **(E)** Bar chart of adenosine concentrations per mouse (WT: n = 7 mice, slices 8, electrodes 45, 304 ± 30 nM; KO: n = 6 mice, 7 slices, electrodes 28, 197 ± 38 nM). CA, cornus ammonis; fEPSP, field excitatory postsynaptic potential; MF, mossy fibers; sp., stratum pyrimdale; sr, stratum radiatum.

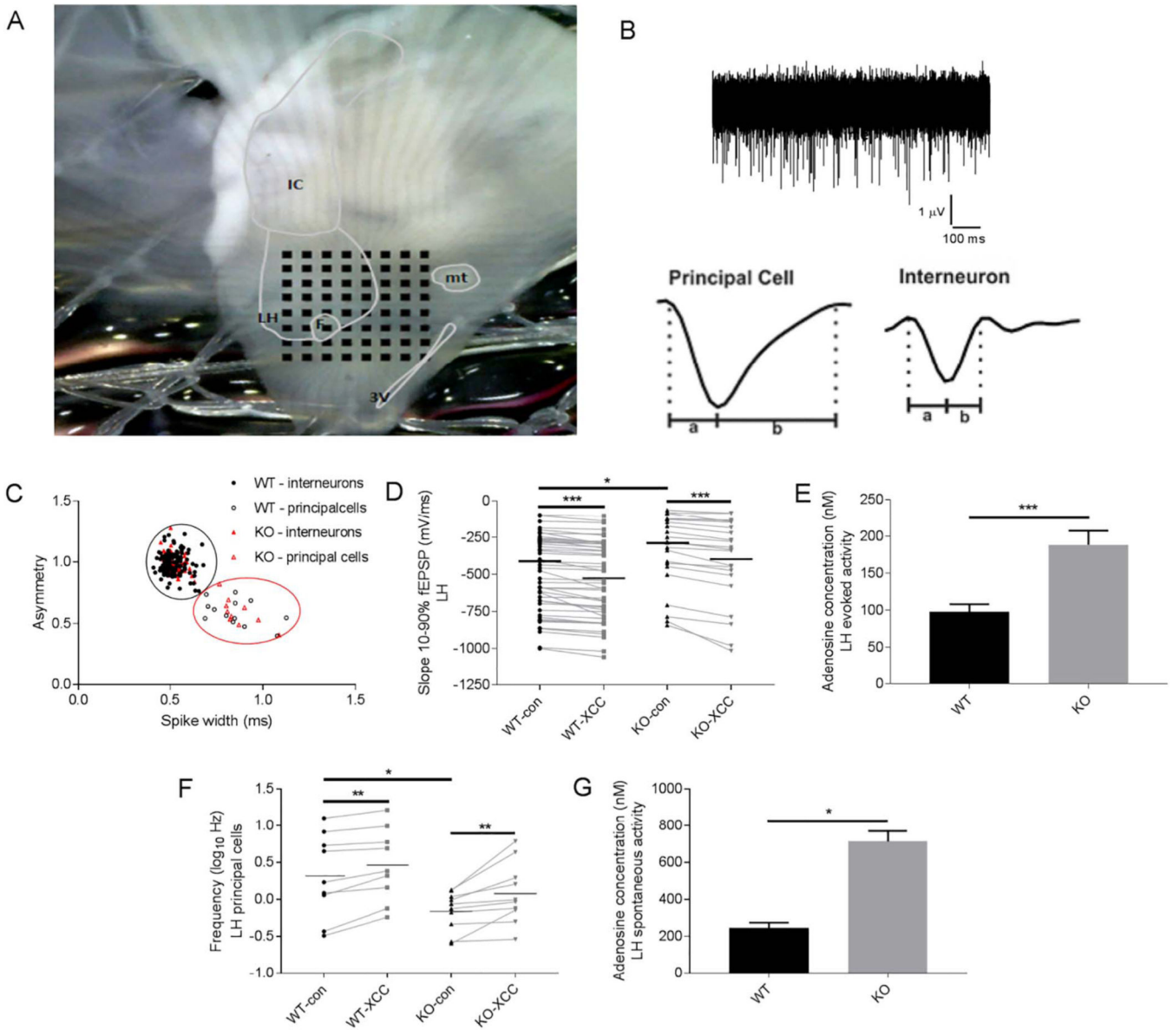

Fig. 5.

Evoked and spontaneous activity of putative orexin neurons is down with increased adenosine levels in KO LH.

(A) Example of coronal slice with 8 × 8 MEA placed over the LH. **(B)** Example trace of spontaneous activity in the LH. Top trace is a 300 s recording. Below, examples of individual principle cell and interneuron waveforms used to determine principal component parameters. **(C)** Principal component analysis of waveforms distinguish principal cells from interneurons based on spike asymmetry (a/b) and spike width (a + b). WT: n = 3 mice, 6 slices, 200 electrodes; KO $n = 4$ mice, 9 slices, 197 electrodes. **(D)** Increases in the slope of fEPSPs from stimulated individual principal cells before and after 10 μM XCC (WT_{con}: −493.8 ± 36 μV/ms v. WT_{XCC}: −525 ± 37 μV/ms, $n = 49$; KO_{con}: −342.4 ± 53 μV/ms v. KO_{XCC}: −396.4 ± 37 μV/ms, $n = 22$, paired t-test). Note: the statistical increase in baseline

fEPSPs of KO compared with WT. **(E)** Adenosine concentration measurements from evoked activity in the LH (WT: 98.09 ± 10.1 nM; KO: 188.7 ± 19.0 nM). **(F)** Spontaneous activity of principal cells before and after A_1R antagonist (WT_{CON}: 3.95 ± 1.4 Hz v. WT_{XCC}: 4.94 ± 1.7 Hz, n = 9 cells; KO_{CON}: 0.80 ± 0.1 Hz v. KO_{XCC}: 1.82 ± 0.6 Hz, n = 10 cells. **(G)** The f.i. was used to calculate the adenosine concentration (WT 243.83 ± 91.3 nM and KO 713.82 ± 177.9 nM). F, fornix; IC, internal capsule; LH, lateral hypothalamus; mt, mamillothalamic tract; MEA, multielectrode array; 3 V, third ventricle.